

Regge oscillations in electron-atom elastic cross sections

D. Sokolovski,¹ Z. Felffi,² S. Yu. Ovchinnikov,³ J. H. Macek,⁴ and A. Z. Msezane²

¹*School of Mathematics and Physics, Queen's University of Belfast, Belfast, BT7 1NN, United Kingdom*

²*Center for Theoretical Studies of Physical Systems, Clark Atlanta University, Atlanta, Georgia 30314, USA*

³*Department of Physics&Astronomy, University of Tennessee, Knoxville, Tennessee 37996, USA*

⁴*Department of Physics&Astronomy, University of Tennessee, Knoxville, Tennessee 37996, USA*

(Received 19 June 2006; published 13 July 2007)

We consider a system trapped in a resonance state, whose decay at zero scattering angle can be related, through the optical theorem, to the total cross section (TCS). We show that for the resonance to contribute to the TCS a peak structure the resonance conditions must be satisfied: (i) Several rotations of the complex (the Regge trajectory—viz., imaginary part versus the real part of the complex angular momentum—stays close to the real axis) and (ii) coherent addition of forward-scattering subamplitudes (the real part of the Regge pole is close to an integer). We exploit the recent complex angular momentum approach of Macek *et al.* [Phys. Rev. Lett. **93**, 183203 (2004)], used to analyze low-energy oscillations observed in the elastic TCS for proton-H scattering, for a detailed analysis of Regge trajectories and their contributions to the TCS in electron-atom scattering for the case of $Z=75$ using the model Thomas-Fermi potential. We conclude by demonstrating through comparison with existing theory and measurements that the Thomas-Fermi potential when used with the appropriate parameters captures the essential physics (Ramsauer-Townsend minima and the Wigner threshold law) in the near-threshold e -Ar and e -Kr elastic scattering.

DOI: [10.1103/PhysRevA.76.012705](https://doi.org/10.1103/PhysRevA.76.012705)

PACS number(s): 34.50.-s, 52.20.Hv, 03.65.Nk

I. INTRODUCTION

Quantum mechanical resonances may affect the outcome of a collision in several ways. In a direct collision, where no resonance is present, the colliding particles part quickly after a brief encounter. If the resonance mechanism plays an important role, the collision partners may form an intermediate complex (diatomic or triatomic, in atom-atom or atom-diatom scattering, or a negative ion if an electron is scattered off a neutral atom), which exists for a certain time before breaking up into its constituent parts. The presence of such a complex can affect both the differential cross section (DCS) and the total cross-section (TCS). A resonant angular distribution results, typically, from the interference between the direct scattering amplitude (which, semiclassically, can be imagined as coming from direct scattering trajectories) and the resonance component produced by the rotation of the decaying intermediate complex. The latter can, therefore be represented by an exponential decaying with the angle φ by which the complex has rotated.

Regge poles—singularities of the S matrix in the complex angular momentum (CAM) plane, which rigorously define scattering resonances—have been studied considerably over the years [1,2] in a variety of fields including atomic and molecular theory, and methods have been developed for their accurate calculations. The fact that, at a given energy E , only the angular momenta in a certain narrow range ΔL around, say, some L_{res} lead to the formation of the complex suggests that the S -matrix element, considered a function of the total angular momentum L at a fixed energy E , must have a resonance Regge pole at $L=L_0(E)$ in the first quadrant of the complex L plane, with a real part close to L_{res} and an imaginary part proportional to ΔL . It is convenient, therefore, to formulate the theory of resonance angular scattering in terms of the Regge poles, as has been done—for example, for

atom-diatom collisions [3], while applications of the approach to simple cases of potential scattering can be found in [4]. Whereas interference between the two mechanisms is likely to produce oscillatory patterns in the DCS, these may or may not cancel when summed over all scattering angles. For this reason, the effect a resonance may produce in the TCS requires a further analysis. Such analysis has been recently conducted by Macek *et al.* [5], who related the low-energy oscillations, experimentally observed in scattering of H^+ on H, to the behavior of the resonance Regge poles arising from the bound states supported by the interatomic potential. Macek *et al.* applied Regge pole analysis directly to the partial wave sum for the TCS, giving for the latter a simple decomposition, similar to the one previously derived, in a different context, by Mulholland [6].

The analysis in Ref. [5] is in terms of Regge trajectories—viz., the graphs of $\text{Im}[L_0(E)]$ vs $\text{Re}[L_0(E)]$. These are easily understood for negative energies, $E < 0$. Mathematically, the pole of the S matrix occurs at $L=L_0$ such that the solution of the Schrödinger equation, regular at the origin, contains as $r \rightarrow \infty$ only the outgoing wave $\exp(ikr)$, $k \equiv (2mE)^{1/2}$, with m being the mass. For $E < 0$ the exponential decays and the regular solution is essentially a bound state. Now, for an arbitrary E one may adjust the real value of L and, therefore, the centrifugal potential $L(L+1)/r^2$ so that the bound state labeled n th in the original ($L=0$) potential has now precisely the energy E . The value of L thus found is the required pole position. The centrifugal term tends to make the effective potential well shallower, so the larger (but still negative) energies require larger L 's and the n th Regge trajectory moves along the real L axis towards greater L 's. For $E > 0$ the analysis is similar, if less intuitive. As the energy becomes positive, the n th Regge pole does not disappear, but acquires a positive imaginary part, so that the complex-valued effective potential emits particles, as re-

quired by the boundary condition, in which $\exp(ikr)$ now represents a traveling wave. Thus, the Regge trajectory leaves the real L axis and veers into the first quadrant of the complex L plane. Macek *et al.* observed that a structure in the TCS, $\sigma(E)$, appears at those energies where at least one Regge trajectory passes in the vicinity of the real integer L value, $\text{Re } L_n(E) \approx 0, 1, 2, \dots, \text{Im } L_n(E) \ll 1$. With each Regge trajectory studied in Ref. [5] passing near an integer value only once and at well-separated energies, the total number of oscillations observed in the σ vs E graph equals that of the bound states in the interatomic potential.

It is natural to ask whether this simple and elegant analysis can be applied to predict and explain low-energy structure in the TCS for light particle collisions, such as the scattering of an electron by a neutral atom or an ion. One expects certain similarities between the two cases. For an electron, the source of the bound states giving rise to Regge trajectories is the attractive Coulomb well it experiences near the nucleus. By adding the centrifugal term to the well one would “squeeze” these states into the continuum in much the same way as happens for the interatomic potential studied in Ref. [5]. The regularity with which the Regge trajectories pass near real integer L 's and, therefore, the pattern observed in the TCS are likely, however, to be different.

The purpose of this paper is to provide a simple and detailed illustration of the use of the Regge pole analysis in general. Specifically, we analyze, within the simplest approximation, the low-energy behavior of the TCS for a Thomas-Fermi potential [7] designed to mimic the interaction between an electron and a neutral atom. The rest of the paper is organized as follows. In Sec. II we rederive the Mulholland formula used in [5] and show that the “passing-near-an-integer” condition, necessary for a Regge trajectory to contribute to the total scattering cross section, amounts to the requirement that the forward-scattering subamplitudes resulting from multiple rotations of the resonance complex add constructively. In Sec. III we analyze in detail the behavior of the Regge trajectories and their contributions to the TCS for a particular system for the purpose of illustrating the method. Sections IV and V contain the dependence of Regge trajectories on nuclear charge and the summary and conclusions, respectively.

II. MULHOLLAND FORMULA AND MULTIPLE ROTATIONS OF THE RESONANCE COMPLEX

We are interested in the total scattering cross section obtained by summing partial cross sections over all (integer) values of the angular momentum (atomic units are used throughout the paper):

$$\sigma_{tot} = 2\pi k^{-2} \sum_{L=0}^{\infty} (L+1/2) |1 - S(E)|^2. \quad (1)$$

Consider next a system trapped in a resonance state formed by the collision partners. The intermediate complex must rotate in order to preserve its angular momentum, this rotation being accompanied by a decay. The effect of this decay on the scattering amplitude $f(\theta)$ at the zero scattering angle θ

$=0$, which is related to the total cross section σ_{tot} through the optical theorem [8]

$$\sigma_{tot} = 4\pi k^{-1} \text{Im}[f(0)]. \quad (2)$$

If the complex has a long (angular) life, it will return to the forward direction many times. This does not, however, guarantee that its decay would produce a significant contribution to σ_{tot} as the subamplitudes corresponding to different numbers of complete rotations may add destructively and cancel one another. The contribution will, nonetheless, be significant if the subamplitudes corresponding to all multiple rotations add constructively—i.e., if the phase acquired in one rotation is close to 2π . This suggests that to see a resonance peak in the dependence of σ_{tot} on E requires that (i) the complex be able to complete several rotations before it breaks up and (ii) there be a coherent addition of forward-scattering subamplitudes.

A mathematical justification for the above can be obtained by applying the Poisson sum formula [9] directly to the right-hand side of Eq. (2), where the forward-scattering amplitude can be written as a partial-wave sum

$$f(\theta) = (ki)^{-1} \sum_{L=0}^{\infty} (L+1/2) [1 - S^L(E)] P_L(\cos(\theta)), \quad (3)$$

with $P_L(\cos(0))=1$ for all L 's. To replace the summation in Eq. (3) by integration we write

$$\sum_{L=-\infty}^{\infty} \delta(\lambda - L - 1/2) = \sum_{m=-\infty}^{\infty} \exp[im\pi(2\lambda + 1)], \quad (4)$$

where $\delta(z)$ is the delta function, and insert it into Eq. (2), which yields

$$\sigma_{tot} = 2\pi k^{-2} \sum_{m=-\infty}^{\infty} \int_0^{\infty} d\lambda \lambda [1 - S(\lambda)] \exp[im\pi(2\lambda + 1)]. \quad (5)$$

In Eq. (5) the $m=0$ term corresponds to replacing the sum in Eq. (2) by an integral and will be left in its present form. For the $m>0$ and $m<0$ terms, the contour of integration can be transformed to run along an arc of large radius in the first and fourth quadrants of the λ plane and then return to the origin down and up the imaginary λ axis, respectively. Since the S matrix has Regge poles at $\lambda_n = L_n + 1/2$ in the first quadrant, closing the contour of integration for the $m>0$ terms will also produce the residue contributions

$$f_{n,m} \equiv -4\pi^2 k^{-2} \lambda_n \text{Res}_n S \exp[im\pi(2\lambda_n + 1)], \quad m = 1, 2, \dots, \quad (6)$$

where $\text{Res}_n S$ is the residue of the S -matrix element at the n th pole. The subamplitudes $f_{n,m}$ have the standard interpretation, at least for the resonance poles located close to the real axis [4]. They describe the decay, in the forward direction, of the intermediate complex associated with the n th resonance poles after completing m full rotations since it has been formed. The real part of the exponent $\pi(2\lambda_n + 1)$ determines the relative phases of individual contributions, while its

imaginary part sets the rate of the angular decay of the complex.

Finally, using the geometrical progression formula to evaluate the sum over multiple rotations,

$$\sum_{m=1}^{\infty} \exp[im\pi(2\lambda + 1)] = -1/[\exp(-i2\pi\lambda) + 1], \quad (7)$$

and taking the imaginary part of the forward-scattering amplitude, we arrive at the Mulholland formula [6] employed in [5]:

$$\sigma_{tot}(E) = 4\pi k^{-2} \int_0^{\infty} \text{Re}[1 - S(\lambda)]\lambda d\lambda - 8\pi^2 k^{-2} \sum_n \text{Im} \frac{\lambda_n \text{Res}_n S}{1 + \exp(-2\pi i\lambda_n)} + I(E), \quad (8)$$

where $I(E)$ contains the contributions from the integrals along the imaginary λ axis. After some algebra, it may be cast in the form

$$I(E) = -4\pi/k^2 \text{Re} \int_0^{i\infty} \frac{\lambda[2 - S(\lambda) - S(-\lambda)]}{1 + \exp(-2\pi i\lambda)} d\lambda. \quad (9)$$

Equation (8) still differs from Eq. (2) of Ref. [5] in that it involves $[1 - S(\lambda)]$ in place of the squared magnitude of the T matrix, $T^2 \equiv |1 - S(\lambda)|^2$. It is, however, easy to demonstrate that the two forms are equivalent. Indeed, from the unitarity of the S matrix on the real λ axis, $S(\lambda) = \exp[i\delta(\lambda)]$, it follows that

$$\text{Re}(1 - S) = |1 - S|^2/2,$$

which establishes the equivalence of the two integral terms. Further, Eq. (2) of [5] uses the residue of the quantity which on the real λ axis is $|1 - S|^2$. Analytical continuation of $|T(\lambda)|^2$ is given by $[1 - S(\lambda)][1 - S^*(\lambda^*)]$. As $S(\lambda)$ has a zero at $\lambda = \lambda_n^*$, its Hermitian conjugate $S^*(\lambda^*)$ has a zero at $\lambda = \lambda_n$ so that

$$\text{Res}_n\{[1 - S(\lambda)][1 - S^*(\lambda^*)]\} = \text{Res}_n\{1 - S(\lambda)\} = -\text{Res}_n S$$

which shows that the two residue terms are also identical.

In the following we will assume $I(E)$ to be small due to the rapid decrease of the integrand for large $|\lambda|$ and will omit it from further discussion. Of the two remaining terms in Eq. (8) the first one is the smooth impact parameter-type contribution, one that is obtained by replacing the summation in Eq. (1) by an integration [5]. The second term describes additional resonance contributions to the first smooth term, which may arise from the poles in the first quadrant of the complex λ plane. From the above discussion it is readily seen that a contribution from the n th pole would be significant if there is a sufficiently large number of subamplitudes in Eq. (5)—i.e., if the complex exists long enough to return to the forward direction many times, which, in turn, requires

$$\text{Im} \lambda_n \ll 1. \quad (10)$$

It is also necessary for these contributions to add constructively—i.e., in phase—so that

$$\text{Re} \lambda_n \approx 1/2, 3/2, 5/2, \dots \quad (11)$$

Thus, as was shown by Macek *et al.*, a resonance is likely to affect the total elastic cross section when its Regge pole position is close to a real integer.

Note the similarity between this condition and the one for the existence of a bound state. Indeed, at a negative energy, a bound state requires $L=0, 1, 2, \dots$, so that the angular part of the wave function retains its value after increasing the value of the azimuthal angle by 2π [10]. Thus, for $E < 0$ a true bound state is found each time a Regge trajectory passes through an integer L (half-integer λ). At positive energies, the passage of a Regge trajectory near an integer point provides an additional condition for the corresponding long-lived resonance to affect the total scattering cross section. One can say that the resonance effect is observed when a particle is trapped in a quasibound state which resembles, both in its radial and angular dependence, a true bound state of the system. In the next section we apply the Mulholland formula in Eq. (8) to elastic scattering by an electron by the Thomas-Fermi (TF) potential [7].

III. RESONANCES AND REGGE TRAJECTORIES FOR A THOMAS-FERMI POTENTIAL

The Thomas-Fermi potential is defined through the solution of the TF equation [7], a delicate nonlinear problem with unusual boundary conditions [11]. The importance of the TF theory, considered as one of the cornerstones of atomic physics [12], is its exactness for atoms, molecules, and solids in the $Z \rightarrow \infty$ limit [13] and that all neutral atoms can be described within the TF model by the universal TF function [14]. Lieb and Simon [12], [13] have investigated extensively the TF theory, including its approach to quantum theory as the number of electrons approaches infinity. The TF potential has been used also to predict reliably [10] the appearance of electrons in the p , d , and f subshells at Z of 5, 21, and 58, respectively as well as to calculate the scattering length for low-energy elastic electron scattering by atoms using an approximate TF potential [15], similar to the one used here, which is taken from Ref. [16].

In order to describe, in the simplest approximation, scattering of an electron by a neutral atom, we employ the one-particle Thomas-Fermi potential of the form [16]

$$U(r) = \frac{-Z}{r(1 + aZ^{1/3}r)(1 + bZ^{2/3}r^2)}, \quad (12)$$

where Z is the nuclear charge and a and b are adjustable parameters. For small r 's, the potential describes the Coulomb attraction between an electron and a nucleus, $V(r) \approx -Z/r$, while at large distances it mimics the polarization potential, $V(r) \approx -1/(abr^4)$. For illustrational purposes we have chosen the parameters

$$Z = 75, \quad a = 0.25, \quad b = 0.06. \quad (13)$$

The effective potential

$$V(r) = U(r) + L(L+1)/r^2 \quad (14)$$

is shown in the three-dimensional plot in Fig. 1 versus r and L , considered here a continuous variable. For $L=0$, $V(r)$ is a

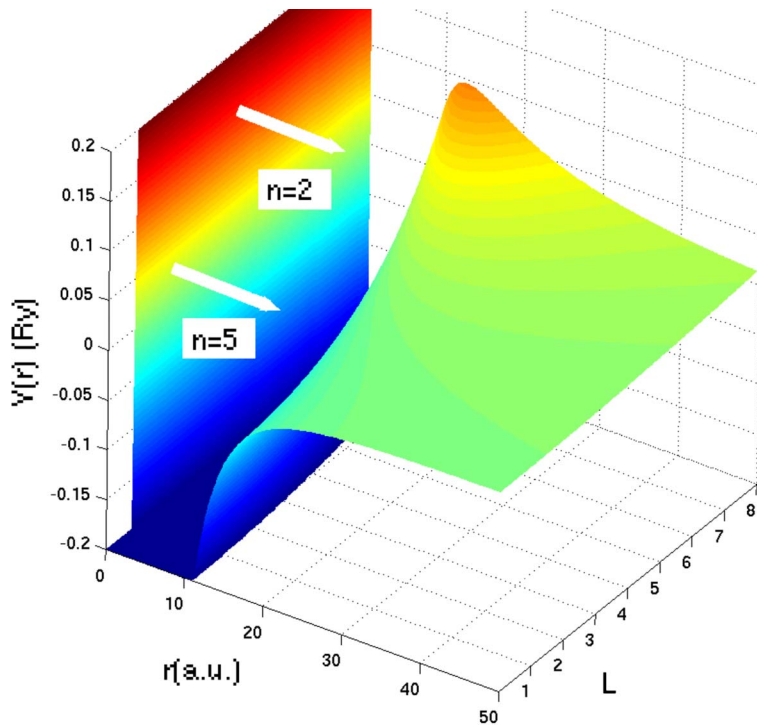


FIG. 1. (Color online) Effective potential $V(r)=U(r)+L(L+1)/r^2$ versus r and L . The bars show the positions of the Regge states with $n=2$ and $n=5$.

potential well which, due to its short-ranged, $\sim 1/r^4$, asymptotic behavior supports a finite number (eight) of bound states, shown in Fig. 2. Figure 1 can be used to illustrate the evolution of bound states supported by the effective potential $V(r)$ as the centrifugal barrier is added to $U(r)$. As L increases, the well becomes shallower; the bound states move upwards and are, eventually, squeezed into the continuum. For larger L 's the effective potential develops a barrier. Thus, a bound state which crosses the threshold $E=0$ in this region may continue to be separated by a barrier—i.e., becomes a long-lived metastable state and continuing that

way until it passes the barrier top. Finally, for even larger L , $V(r)$ becomes purely repulsive and no longer supports narrow resonances.

We will, however, consider the diagram Fig. 1 from a different perspective; i.e., we fix the value of the energy E and ask for the value of the angular momentum $L_n(E)$ required to make the energy of the n th state, $E_n(L)$, equal to E . For $E < 0$, the value of L_n required to “tune” $E_n(L)$ to E is real while for positive energies it is complex valued. Note that one must have $\text{Im} L_n > 0$ so that the complex-valued centrifugal barrier emits particles, as the Regge states contain

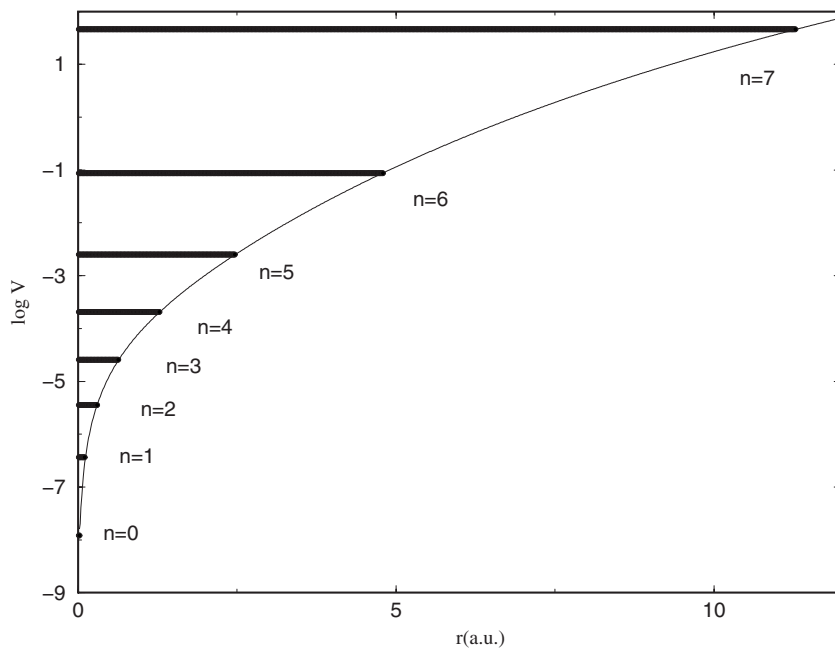


FIG. 2. The eight bound states supported by the Thomas-Fermi potential for $Z=75$. A logarithmic scale is used to allow for better viewing.

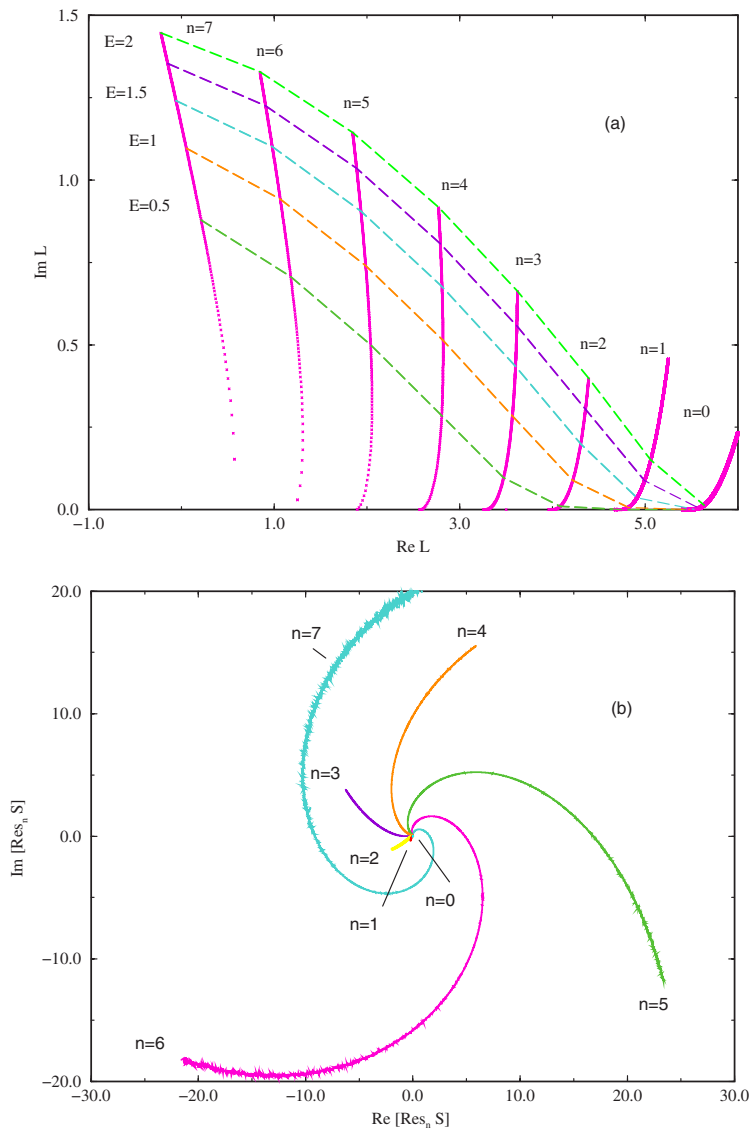


FIG. 3. (Color online) (a) Regge trajectories associated with the $L=0$ bound states shown in Fig. 2. The dashed lines indicate the respective Regge poles positions at a given value of E (Ry). (b) Residue trajectories [17] $\text{Im}[\text{Res}_n S]$ versus $\text{Re}[\text{Res}_n S]$ for $n=0, 1, \dots, 8$.

for large r 's an outgoing traveling wave. For positive energies below the top of the effective barrier $\text{Im} L_n$ should remain small for the corresponding metastable states. As the energy increases above the barrier top, all (in our case 8) L_n acquire significant imaginary parts and there are no more resonances. Plotting $\text{Im} L_n$ versus $\text{Re} L_n$ rather than $\text{Im} L_n$ and $\text{Re} L_n$ versus E , one obtains Regge trajectories [5,17]. Thus, a typical trajectory associated with the n th bound state of $U(r)$ runs along the real L axis for as long as the energy remains negative and, for $E > 0$, departs from the real axis, slowly or more rapidly, depending on the effective potential encountered by the bound state emerging from the well. The condition that all the Regge trajectories will have left the real L axis sets the energy range within which the total cross section can be influenced by the resonances.

The eight Regge trajectories originating from the bound states in Fig. 1 are shown in Fig. 3(a), with the rightmost one corresponding to the ground state of $U(r)$. Note that the magnitudes of the residues steadily increase with energy. The pole positions and residues were obtained by the method

similar to that of Burke and Tate [18]—i.e., by numerically integrating the radial Schrödinger equation for complex values of the total angular momentum and searching for the zeros of the coefficient multiplying the incoming wave. An alternative semiclassical approach to calculating Regge trajectories for the TF potential can be found in Ref. [16].

Like the Regge trajectories reported in Ref. [5], those in Fig. 3(a) are almost uniformly spaced along the real L axis. The spacing is, however, not an integer, so that only the $n=2$ and $n=5$ trajectories pass near integer values of $L=4$ and $L=2$, respectively. The $n=2$ trajectory does so at an energy $E=0.193$ Ry with $\text{Im} L=0.000165$, while one expects the $n=5$ trajectory with $\text{Im} L=0.0813$ to be responsible for a broader resonance at $E=0.061$ Ry. Thus, if the potential correctly describes an electron-atom collision, Fig. 3(a) predicts the creation of a negative ion in metastable states with $L=4$ and $L=2$ at $E=0.0061$ Ry and $E=0.193$ Ry, respectively. The six remaining trajectories, which do not approach integer values, are expected to have much smaller effect on $\sigma_{\text{tot}}(E)$. The transversal dashed lines in Fig. 3(a) connect the

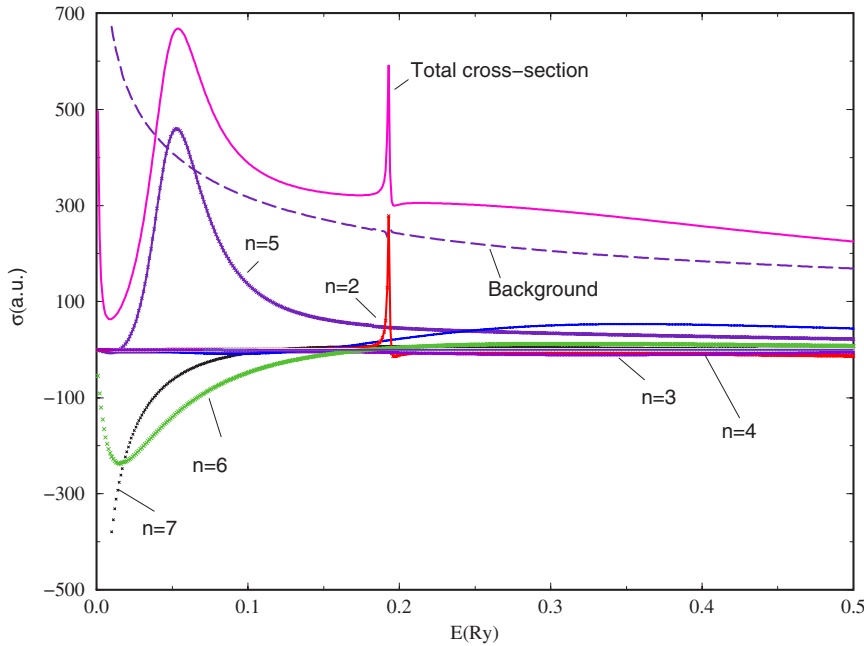


FIG. 4. (Color online) The total elastic cross-section (solid line) versus E (Ry). The individual Mulholland contributions (crosses) and the smooth background (dashed) corresponding to the first term in Eq. (8) are also shown.

positions of the Regge poles for the same $E > 0$. Note that for the trajectories associated with the lower bound states of $U(r)$, $\text{Im} L_n(E)$ remains small even for relatively large E . This behavior is consistent with the observation that for large L 's, $V(r)$ develops a barrier which continues to support long-lived metastable states after a bound state crosses the threshold $E=0$. We will return to this matter shortly. Figure 3(b) shows the “residue trajectories” [17], graphs $\text{Im}(\text{Res}_n S)$ versus $\text{Re}(\text{Res}_n S)$ in the same energy range. Note that the magnitude of a residue steadily increases with energy E and vanishes at $E=0$. Mathematically, this is expressed by the fact that unitarity of the S matrix at the real L axis requires that each Regge pole in the first quadrant of the complex L plane be complemented by a Regge zero located symmetrically in its fourth quadrant. Thus, for a narrow resonance, the residue is necessarily small and for a bound state, which cannot be accessed with a positive energy, $\text{Res}_n S$ is zero.

The total scattering cross section is shown in Fig. 4 in the range $0 < E < 0.5$ Ry, whereas the differential cross section $\sigma(\theta, E)$ is shown in the three-dimensional plot in Fig. 5. In both plots one notices the sharp peak at $E=0.193$ Ry associated with the $n=2$ Regge trajectory. A much broader peak, attributed to the $n=5$ trajectory, is clearly visible near $E \approx 0.061$ Ry. The peak is slightly shifted towards smaller energies, as its position is determined by the number of terms in the geometric progression, Eq. (7), which is larger for smaller energies, as well as the coherence between the phases of individual terms. The contributions of individual Regge states to the sum Eq. (8) in the Mulholland formula are shown in Fig. 4. Note that the trajectories associated with the sixth and seventh excited states ($n=6$ and $n=7$), which do not approach integer values, provide considerable negative contributions responsible for the dip in the total cross section at $E \approx 0.01$ Ry due to the amplifying effect the factor k^{-2} has for small energies.

Finally, one may expect at least the sharp peak at $E = 0.193$ Ry to be associated with a narrow shape resonance

supported by the potential barrier in the effective potential. However, a more detailed analysis shows that this is not the case. The positions of the two ($n=2$ and $n=5$) resonances, in both r and L , are shown in Fig. 1 by white bars. It is readily seen that both energies lie above their respective barrier tops. A better view is provided by Fig. 6(a) which shows the effective potentials, energies, and the corresponding Regge states. The $n=2$ Regge state is large in the well region of $V(r)$ and has a relatively small outgoing wave for large r . This is consistent with the picture of a particle spending a long time in the well before finally escaping. As its energy is well above the barrier, one has to assume that its confinement is caused by the reflection above the steep wall of the potential well. The $n=5$ Regge state in Fig. 6(b) shows no such increase of the density in the well region and, therefore, must be emptied almost immediately after the particles are created by the complex-valued centrifugal potential. Interestingly, for the parameters in Eq. (13) we have found no shape resonances attributable to the effective barrier.

IV. DEPENDENCE OF REGGE TRAJECTORIES ON NUCLEAR CHARGE

A brief discussion of the dependence of the Regge trajectories and total cross sections on the nuclear charge Z is appropriate. For this purpose, we have selected the values $Z=18, 36$, and 54 (Fig. 7), corresponding to Ar, Kr, and Xe, respectively. As the charge Z increases, the $L=0$ potential well becomes deeper and one expects it to support more bound states giving rise to more Regge trajectories. Indeed, for $Z=18$ we find six such trajectories, while for $Z=36$ their number increases to 7 and for $Z=54$ it becomes 8, as shown in Figs. 8(a), 8(b), and 8(c). As in Fig. 3(a) the trajectories are labeled according to the number of the bound state that they are associated with, with the furthestmost on the right coming from the ground state $n=0$. The corresponding Mulholland contributions to the $Z=18, 36$, and 54 total cross

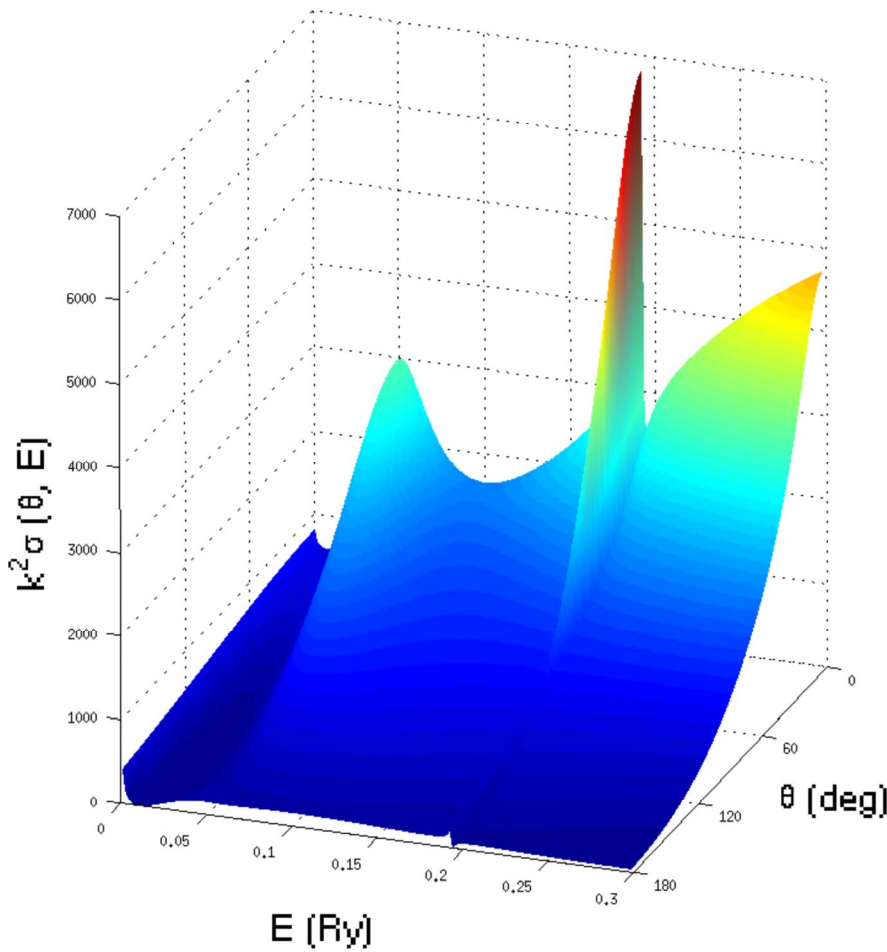


FIG. 5. (Color online) The differential cross section $\sigma(\theta, E)$ versus θ (deg) and E (Ry).

sections are shown in Figs. 8(a), 8(b), and 8(c). We note that, in general, the nearly equal spacings between the trajectories are not equal to integers, so that not all trajectories contribute to the structure in the total cross section. The latter may, therefore, have or not have sharp resonances as well as

broader features associated with the Regge poles. Note also that none of the trajectories approach more than one integer value of L so that none of the Mulholland contributions contain more than one maximum, as is the case, for example, for elastic scattering of protons by neutral atoms.

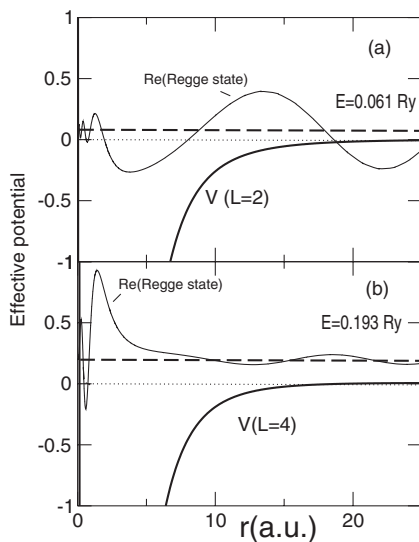


FIG. 6. Effective potentials and energies (Ry) for the two Regge states: (a) corresponds to the state with $n=5$, $L=2$, and $E=0.061$ Ry, while (b) to that with $n=2$, $L=4$, and $E=0.193$ Ry.

We have also carried out a careful investigation of the near-threshold behavior of the elastic scattering cross sections with respect to the variation of the parameters of the TF potential for e -Ar and e -Kr scattering to assess the robustness of the Thomas-Fermi potential. We focused specifically upon the position and magnitude of the Ramsauer-Townsend (RT) minima and the Wigner threshold behavior, comparing the former results with those of the recent careful theoretical investigations of Savukov [22] and the attendant measurements [23,24]. One reason for our investigation is that Ar ($Z=18$) appears to be on the low side for the applicability of the TF model, while the other is that the Savukov calculations used the many-body perturbation theory (MBPT) method to calculate the energies for the Ar^- and Kr^- ions and obtained accurate elastic scattering cross sections for both e -Ar and e -Kr beyond Hartree-Fock using the Brueckner-orbital approximation. Comparison of our calculated data with those of Savukov and others may indicate the importance or unimportance of many-body effects.

In Fig. 9(a) we show the variation of σ_{tot} with E (eV) for e -Ar scattering for values of $b=0.04$, 0.045, and 0.046 to determine the robustness of σ_{tot} with respect to the polarization potential. The figure shows the sensitivity of the σ_{tot}

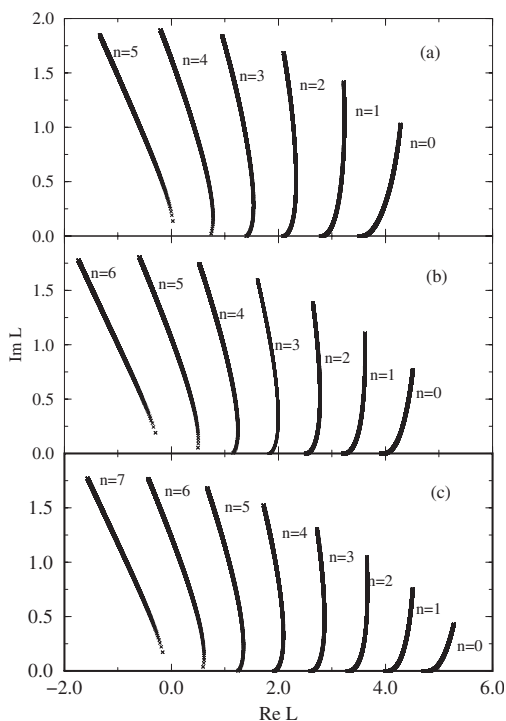


FIG. 7. Regge trajectories for $Z=18$, $Z=36$, and $Z=54$ shown in (a), (b), and (c), respectively.

with respect to the variation in the TF potential. Clearly the optimal value for the parameter corresponds to 0.045, yielding the desired RT minimum; note that the value of 0.046 leads to spurious behavior in the elastic cross section. The values we obtained for the position and magnitude of the minimum are about 0.45 eV and $0.3 \times 10^{-20} \text{ m}^2$, respectively. These values compare well with those read from the Savukov paper: 0.36 eV and $0.3 \times 10^{-20} \text{ m}^2$, respectively. Because of the close agreement between our values of the position and the magnitude of the minimum and those of Savukov and the measurements [23,24], we may infer that many-body effects are not as important as the polarization effects at near-threshold impact energies in the e -Ar scattering.

Similarly, we also investigated the effect of the variation of the b parameter on the RT minimum in the e -Kr elastic scattering cross section. Figure 9(b) compares the elastic total cross section σ_{tot} , corresponding to the values of $b = 0.0285, 0.029, 0.031, 0.032, \text{ and } 0.033$. We found the RT minimum to be between 0.35 and 0.55 eV and its value to be between $0.4 \text{ and } 0.9 \times 10^{-20} \text{ m}^2$ when we used the values of b between 0.0285 and 0.032. Those values are within the range of the theoretical data [22,25] and the experimental values [23,26,27], lying between the 0.6 and 0.9 eV range with the value of the minimum lying between $0.4 \text{ and } 0.7 \times 10^{-20} \text{ m}^2$.

Our main aim in these paragraphs was to demonstrate that the TF potential, with appropriate parameters, captures the essential physics (RT minima—their positions and values—as well as the Wigner threshold law) in the near-threshold e -Ar and e -Kr elastic scattering. In both e -Ar and e -Kr scattering an s -wave Wigner threshold law is followed,

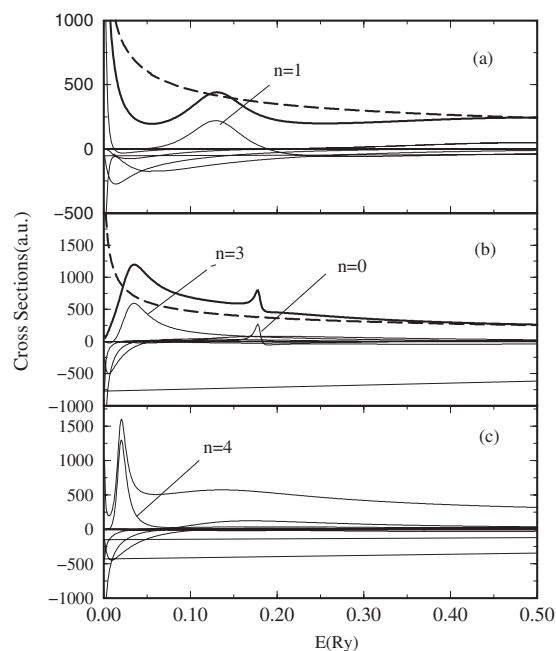


FIG. 8. The total elastic cross section (thick solid) versus E (Ry). The individual Mulholland contributions (solid) and the smooth background (dashed) corresponding to the first term in Eq. (8) are also shown in (a), (b), and (c) for $Z=18, 36$, and 54 , respectively.

consistent with the expected behavior and the finding of Savukov.

The Regge trajectories, obtained within the complex angular momentum representation of scattering and presented in this paper, have been employed recently for a fundamental understanding of the near-threshold electron attachment in e^- -Fr and e^- -Cs collisions [19], capturing, with considerably less effort and unambiguously, the essential results of the Dirac R matrix [20] and predicting new manifestations. The present method has also been employed to provide insight into developing resonances and Regge oscillations in the state-to-state integral cross sections of the $F+H_2$ reaction [21].

V. SUMMARY AND CONCLUSIONS

In summary, we have presented a complex angular momentum analysis of low-energy electron-atom scattering considered within the Thomas-Fermi approximation. As in the case of ion-atom collision studied in [5], we found the total cross section $\sigma_{tot}(E)$ to be affected by the Regge trajectories associated with the $L=0$ bound states of the negative ion. However, whereas for the proton impact on hydrogen the structure produced in the total cross section is regular, with each trajectory responsible for just one oscillation, the electron-atom case is more complicated. Even though the trajectories in Fig. 3(a) appear to have regular spacings, only a few of them satisfy the “resonance” condition of “passing near an integer” and produce sharp peaks in $\sigma_{tot}(E)$. The rest either contribute very little or produce broad overlapping

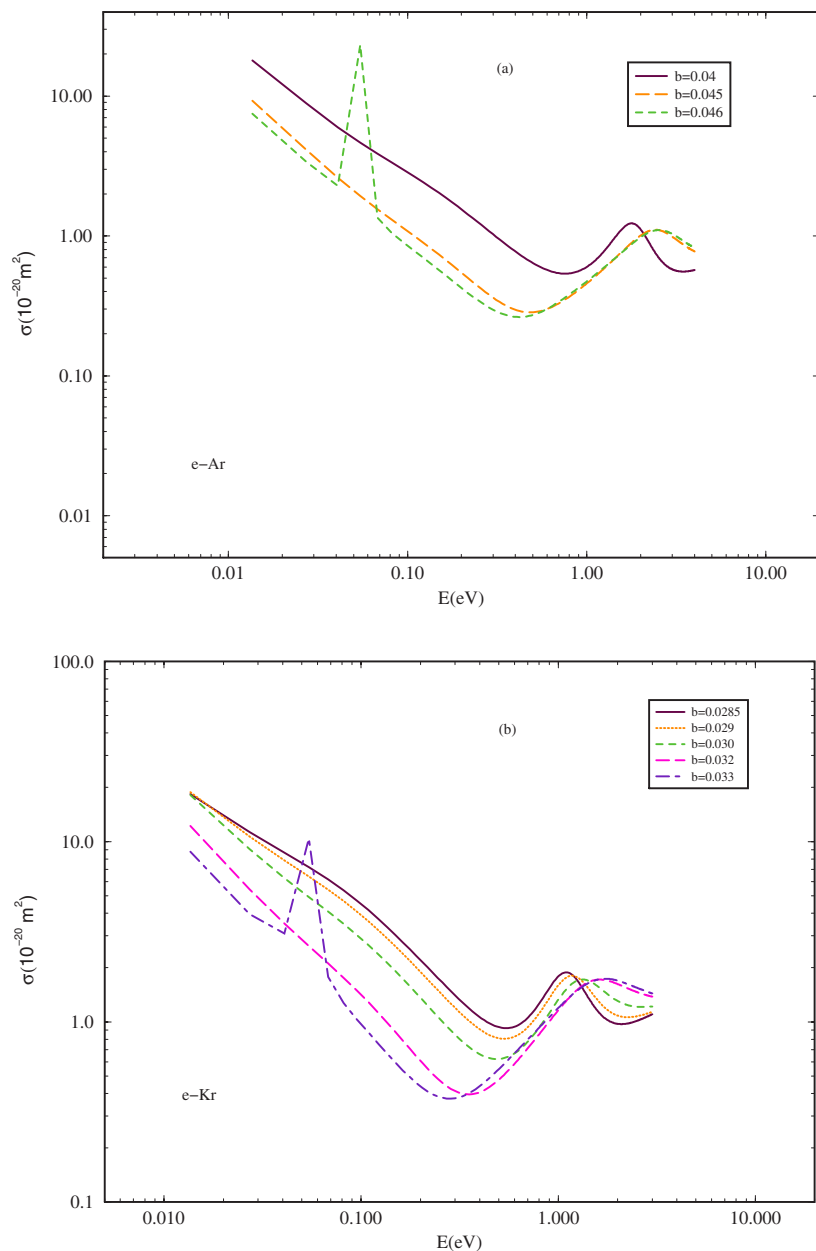


FIG. 9. (Color online) The variation of the total elastic cross section versus E (eV), with the b parameter of the TF potential. (a) shows the results for e -Ar scattering, and (b) presents the data for e -Kr scattering.

peaks or dips. The resulting irregular structure can be analyzed by considering individual resonance contributions superimposed against a smooth background described by the first term of the Mulholland formula, Eq. (8). It is interesting to note that the sharp resonance peaks observed in $\sigma_{tot}(E)$ are not associated with the shape of the barrier top resonances of the effective potential. Rather, we found them located well above the barrier top and, most likely, supported by the reflection over the edge of the potential well. While we believe our general conclusions to be accurate, further progress can be made by optimizing the effective one-electron potential and comparing the results with those from the more sophisticated multichannel R -matrix calculations [28].

We conclude by noting that the strength of our method is that it allows for a close scrutiny of the elastic threshold

energy region, as well as the identification without ambiguity of the angular momenta responsible for the various structures in the total elastic cross section, limited only by the nature of the interaction chosen. We are currently working on refining our potential so that it would reflect certain measurable quantities for a given atomic system (e.g., the parameters a and b optimized to yield the dipole polarizability of the atom in the limit $r \rightarrow \infty$). The next step will be to extend the Regge approach to the interesting and challenging multichannel case.

ACKNOWLEDGMENTS

This work was supported by U.S. DOE, Division of Chemical Sciences, Office of Basic Energy Sciences, Office of Energy Research and AFOSR. The authors wish to thank N. B. Avdonina for valuable discussions.

- [1] S. C. Frautschi, *Regge Poles and S-matrix Theory* (W. A. Benjamin, New York, 1963), Chap. X.
- [2] V. de Alfaro and T. Regge, *Potential Scattering* (North-Holland, Amsterdam, 1965).
- [3] D. Sokolovski and J. F. Castillo, *Phys. Chem. Chem. Phys.* **2**, 507 (2000); D. Sokolovski, *Chem. Phys. Lett.* **370**, 805 (2003).
- [4] D. Sokolovski and A. Z. Msezane, *Phys. Rev. A* **70**, 032710 (2004).
- [5] J. H. Macek, P. S. Krstic', and S. Yu. Ovchinnikov, *Phys. Rev. Lett.* **93**, 183203 (2004).
- [6] H. P. Mulholland, *Proc. Cambridge Philos. Soc.* **24**, 280 (1928).
- [7] L. H. Thomas, *Proc. Cambridge Philos. Soc.* **23**, 542 (1924); *E. Fermi, Z. Phys.* **48**, 73 (1928).
- [8] S. Geltman, *Topics in Atomic Collision Theory* (Krieger, Malabar, FL, 1997), p. 13.
- [9] D. M. Brink, *Semi-Classical Methods in Nucleus-Nucleus Scattering* (Cambridge University Press, Cambridge, England, 1985).
- [10] L. D. Landau and E. M. Lifshitz, *Quantum Mechanics (Non-Relativistic Theory)* (Butterworth-Heinemann, Oxford, 1999), Vol. 3, p. 277.
- [11] L. N. Epele, H. Fanchiotti, C. A. Garcia Canal, and J. A. Ponceano, *Phys. Rev. A* **60**, 280 (1999).
- [12] E. H. Lieb, *Rev. Mod. Phys.* **53**, 603 (1981); **54**, 311(E) (1982).
- [13] E. H. Lieb and B. Simon, *Adv. Math.* **23**, 22 (1977); *Phys. Rev. Lett.* **31**, 681 (1973).
- [14] L. Spruch, *Rev. Mod. Phys.* **63**, 151 (1991).
- [15] T. Z. Tietz, *Z. Naturforsch. A* **26**, 1054 (1971).
- [16] S. Belov, N. B. Avdonina, Z. Felfli, M. Marletta, A. Z. Msezane, and S. N. Naboko, *J. Phys. A* **37**, 6943 (2004).
- [17] J. N. L. Connor, *J. Chem. Soc., Faraday Trans.* **86**, 1627 (1990); *Mol. Phys.* **23**, 717 (1972).
- [18] P. G. Burke and C. Tate, *Comput. Phys. Commun.* **1**, 97, (1969).
- [19] Z. Felfli, A. Z. Msezane, and D. Sokolovski, *J. Phys. B* **39**, L353 (2006).
- [20] C. Bahrim, U. Thumm, and I. I. Fabrikant, *Phys. Rev. A* **63**, 042710 (2001).
- [21] D. Sokolovski, D. de Fazio, S. Cavalli, and V. Aquilanti, *J. Chem. Phys.* **126**, 121101 (2007).
- [22] I. M. Savukov, *Phys. Rev. Lett.* **96**, 073202 (2006).
- [23] Y. K. Gus'kov, R. V. Savvov, and V. A. Slobodyanyuk, *Zh. Tekh. Fiz.* **48**, 277 (1978).
- [24] S. J. Buckman and B. Lohmann, *J. Phys. B* **19**, 2547 (1986).
- [25] B. Plenkiewicz, P. Plenkiewicz, C. Houée-Levin, and J.-P. Jay-Gerin, *Phys. Rev. A* **38**, 6120 (1988).
- [26] S. J. Buckman and B. Lohmann, *J. Phys. B* **20**, 5807 (1987).
- [27] K. P. Subramanian and V. Kumar, *J. Phys. B* **20**, 5505 (1987).
- [28] K. A. Berrington, W. Eissner, and P. N. Norrington, *Comput. Phys. Commun.* **92**, 290 (1995).